Progress In Electromagnetics Research Letters, Vol. 52, 121–128, 2015

Hexa-band High-Isolated Dual-Polarized Loop Antenna for Mobile Communications

Changjiang Deng, Yue Li*, Zhijun Zhang, and Zhenghe Feng

Abstract—This paper presents a broadband hexa-band dual-polarized loop antenna for mobile communications. Two orthogonal one-wavelength-perimeter modes of a rectangular loop are excited by two orthogonal feedings. One mode for vertical polarization is excited by a circular monopole, and the other mode for horizontal polarization is excited by a slot-coupled microstrip line. By optimizing the antenna structure and the orthogonal feedings, the orthogonal polarizations can be achieved in a wide bandwidth with high ports isolation. The overall size of the proposed antenna is only $58 \times 53\,\text{mm}^2$ ($0.43\lambda_0 \times 0.39\lambda_0$, λ_0 is the free-space wavelength at 2.2 GHz). A prototype of the proposed antenna is built and tested. The measured bandwidth with reflection coefficient less than -10 dB is 61.4% (1.65–3 GHz) for both orthogonal polarizations, covering the DCS, PCS, UMTS, WLAN, LTE2300, and LTE 2500 operation. The measured ports isolation is better than 28 dB over the entire band. In addition, the radiation patterns, gains and diversity performance are also discussed.

1. INTRODUCTION

Driven by high-speed wireless data transmission applications, broadband antennas have attracted more and more research interest. For mobile communication systems, the bandwidth of antennas is required to be wide enough to cover the typical frequency bands, such as DCS (1710–1880 MHz), PCS (1850–1990 MHz), UMTS (1920–2170 MHz), and WLAN (2400–2480 MHz) operation [1]. Recently, new frequency bands, such as LTE2300 (2300–2400 MHz) and LTE2500 (2600–2690 MHz) operation, have been assigned for the new generation (4G). Therefore, a broad bandwidth of 45% (1710–2690 MHz) is desirable to provide services for different mobile communication systems.

Dual-polarized antennas are widely studied and adopted to improve the channel capacity [2]. In the last decades, various dual-polarized antennas have been proposed with different kinds of radiators [3–21]. Dipole antennas [3–6], patch antennas [7–13], dielectric resonator antennas (DRAs) [14, 15], slot antennas [16–19], and loop antennas [20, 21] are the typical radiators. Among them, the slot antennas are a promising candidate to achieve dual polarization since it has the merits of planar structure and broad bandwidth. For example, in [19], a dual-polarized circular slot antenna is proposed for mobile communications. The bandwidth is wide enough to cover the desired 1710–2690 MHz band with high isolation. However, the slot antenna occupies a large size owing that the slot operates at the half-wavelength mode. To further decrease the planar dimensions of the slot antennas, the loop antennas are proposed as an effective solution for dual operation. Considering that the loop antenna operates at the one-wavelength-perimeter mode, the size of the loop antennas is more compact than that of the slot antennas. A comparison between the dual-polarized slot antenna and the loop antenna is made in [21]. It is shown that the size of the loop antenna in [21] is much smaller than that of the slot antenna in [18], while keeping the bandwidth almost unchanged.

Received 22 February 2015, Accepted 30 March 2015, Scheduled 9 April 2015
* Corresponding author: Yue Li (lyee@tsinghua.edu.cn).
The authors are with the Department of Electronic Engineering, Tsinghua University, Beijing 100084, China.

The bandwidth of the loop antenna in [21] is about 30%, which is narrow for mobile communications. In this paper, a compact loop antenna is proposed to broaden the bandwidth. Two orthogonal one-wavelength-perimeter modes of a rectangular loop are excited by two independent feedings for dual polarization. The measured −10-dB bandwidth is 61.4% (1.65∼3 GHz), also with ports isolation less than −28 dB across the bandwidth. Therefore, the bandwidth is sufficient to cover the DCS, PCS, UMTS, WLAN, LTE2300, and LTE 2500 operation. Compared with the design in [21], the proposed antenna has the merits of wide bandwidth and high ports isolation.

2. ANTENNA DESIGN

Figure 1 shows the geometry of the proposed dual-polarized antenna. The designed antenna is printed on a 1-mm-thick FR4 substrate with relative permittivity $\varepsilon_r = 4.4$ and loss tangent $\tan\delta = 0.02$. A ground plane and two microstrip lines are printed on the front and back layers of the substrate, respectively. The ground plane has a wide rectangular slot etched to form a loop structure, and a small open slot etched on the loop for excitation. The microstrip line for port 1 is connected with a circular monopole. The stepped microstrip line for port 2 is placed above the small open slot and is shorted to the ground via a metal pin. The dimensions of the proposed antenna are optimized by Ansoft HFSS version 11.2 and the detailed values are listed in Table 1.

Here, we analyzed the operating principle of the proposed dual-polarized antenna. We selected a rectangular loop as the main radiator to provide dual orthogonal polarizations. Taking the advantage of the symmetry of the loop structure, the dual orthogonal polarizations can be excited by two spatially orthogonal feedings, e.g., a stepped microstrip line and a circular monopole, which are shown in Figure 1. Each polarization operates at the one-wavelength mode of the rectangular loop. Therefore, the mean circumference of the rectangular loop is about 1λ in the dielectric, determined by the operating frequency. As illustrated in Figure 2, the dual orthogonal one-wavelength modes of the rectangular loop can be excited by port 1 (the vertical mode) and port 2 (the horizontal mode). Figure 2 shows the current distribution of the loop with different feeds. In Figure 2(a), the vertical mode of the loop is excited. In this mode, two current nulls appear on the two horizontal arms of the loop. In Figure 2(b), the horizontal mode of the loop is excited. In this mode, the energy is coupled from the

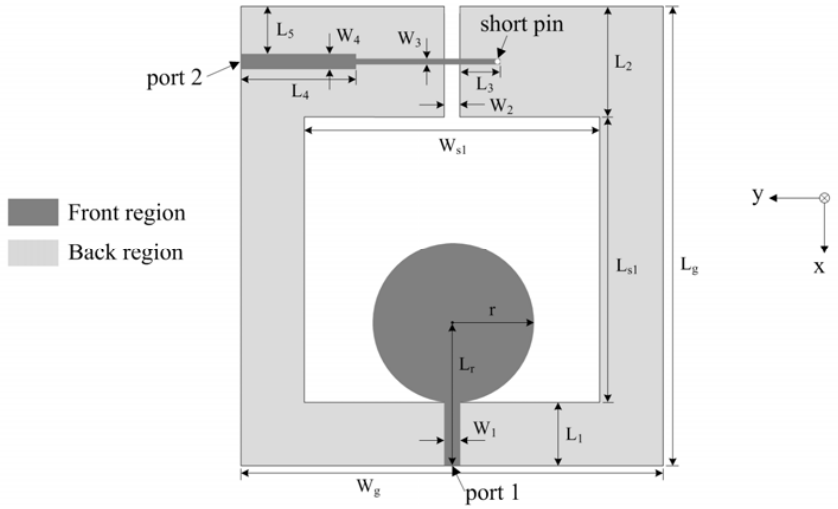

Figure 1. Geometry and dimensions of the proposed antenna.

Table 1. Detailed dimensions (unit: mm).

l_g	w_g	l_1	w_1	l_2	w_2	l_3	w_3	l_4	w_4	l_5	l_{slot}	w_{slot}	r	l_r
58	53	8	2	14	2	18	0.8	14.5	2	6	36	37	10	18

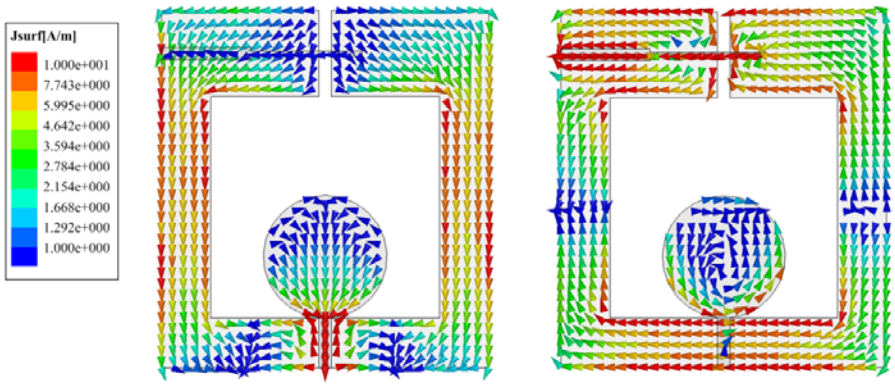

Figure 2. Current distribution of the proposed antenna at 2.2 GHz: fed from (a) port 1; (b) port 2.

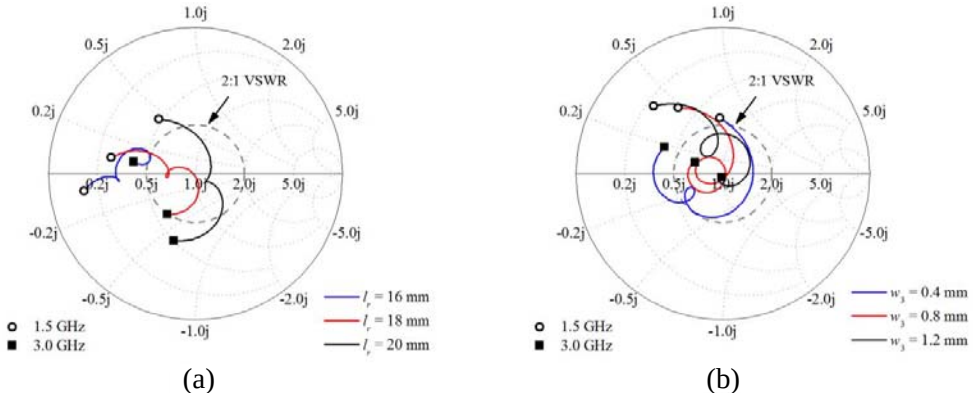

Figure 3. Parameter analysis. (a) S_{11} in Smith chart with different l_r. (b) S_{22} in Smith chart with different w_3.

stepped microstrip line to the open slot. Two current nulls appear on the two vertical arms of the loop. Therefore, the current nulls of the two modes appear on different arms. Then, the mechanism of high isolation between the dual modes is discussed. In Figure 2(a), It is shown that the current intensity on the stepped microstrip line is very small, which indicates few energy is coupled to port 2. In Figure 2(b), the current on the circular microstrip line is observed very weak, which indicates few energy is coupled to port 1. Therefore, high isolation is achieved between the two ports. In addition, small antenna footprint can be obtained by using the rectangular loop structure. This is because that the loop antenna operates at the one-wavelength-perimeter mode. Each arm of the loop has a length of about 0.25λ, as the shape of the rectangular loop in the proposed design approaches to a square loop. In contrast, each arm of the slot antenna is about 0.5λ, considering that the slot antenna operating at the half-wavelength mode.

According to the analysis mentioned above, the general value of each parameter can be calculated. Here, the HFSS software is used to optimize the detailed value of each parameter. The optimization objective is the overlapping bandwidth of the dual orthogonal modes, fed though port 1 and port 2, separately. The size of the loop structure is selected first according to the operating frequency. Due to the symmetry of the antenna structure and spatially orthogonal feedings, the ports isolation is high, as discussed above in Figure 2. Then, the optimization parameters include the radius (r) and offset length (l_r) of the circular monopole for port 1, and the length (l_3 and l_4) and width (w_3 and w_4) of the stepped microstrip line for port 2. Owing to high port isolation, the parameters for the two feedings can be optimized separately. A parametric study of all the parameters is carried out and some key parameters are found to optimize the bandwidth of each port. Figure 3(a) shows the impedance tuning of port 1 in

Smith chart. It can be observed that the impedance can be well matched by only tuning l_r, the offset length of the circular monopole for port 1. Figure 3(b) shows the impedance changes of port 2 in Smith chart. It is shown that the impedance of port 2 is optimized, when w_3 equals 0.8 mm. The above results indicate that the impedance of both ports is well matched by tuning the corresponding parameters of the two feedings. Therefore, the overlapping bandwidth of both ports can be optimized.

3. RESULTS AND DISCUSSION

3.1. *S* Parameters and Radiation Performance

To validate the performance of the proposed loop antenna, a prototype is fabricated and tested, as is shown in Figure 4. Figure 5 shows the simulated and measured S parameters of the proposed antenna. Due to the measurement and fabrication errors, there is a little difference between the simulated and measured results. The measured −10-dB reflection coefficient bandwidth is 1.35 GHz (1.65∼3 GHz) for the vertical mode (port 1) and over 1.4 GHz (1.6∼>3 GHz) for the horizontal mode (port 2). Therefore, the overlapping −10-dB bandwidth for both modes is 61.4%, which covers the desired DCS, PCS, UMTS, WLAN, LTE2300, and LTE 2500 operation. It is worth mentioning that the simulated overlapping bandwidth for both modes is lower than −15 dB (VSWR < 1.5) across the 1710–2690 MHz band. The measured isolation is about −30 dB over the entire band, while the simulated isolation is about −35 dB. This deterioration may be caused by mutual coupling between the two feeding cables. Compared with the loop antenna in [21], the bandwidth of the proposed antenna is improved from 30.4% to 61.4%, and the ports isolation is also improved from −20 dB to −30 dB.

The simulated and measured normalized radiation patterns for port 1 and port 2 are plotted in Figure 6 and Figure 7, respectively. Figure 6 shows the results for port 1 excitation at frequencies of

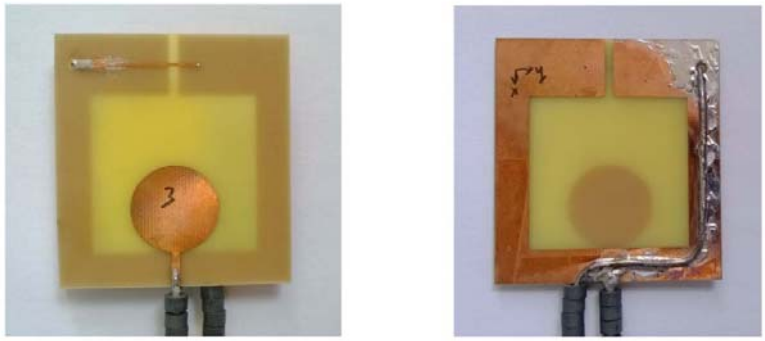

Figure 4. Photos of the manufactured antenna. (a) Front view. (b) Back view.

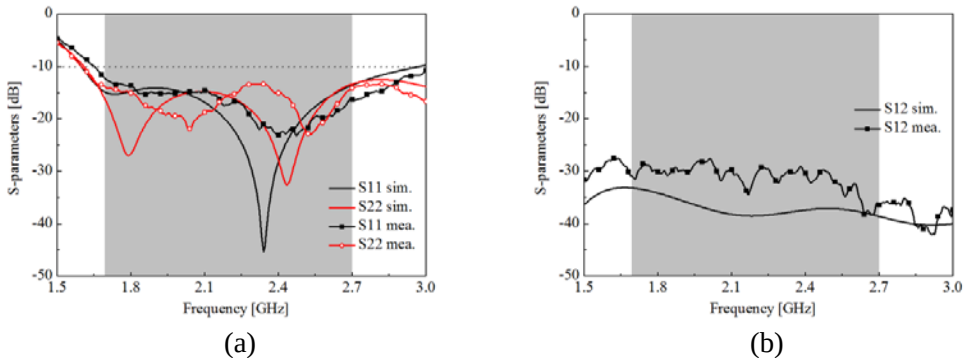

Figure 5. Simulated and measured S parameters. (a) Reflection coefficients. (b) Ports isolation.

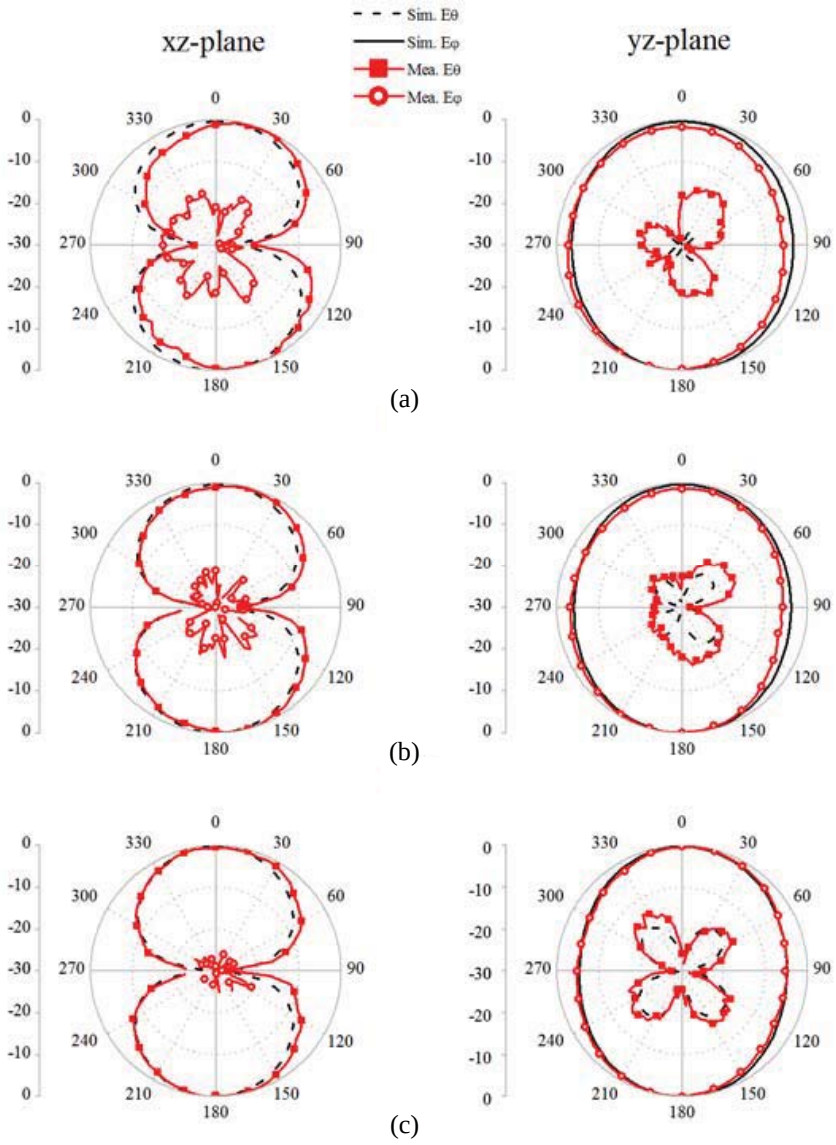

Figure 6. Simulated and measured normalized radiation patterns for port 1 excitation. (a) 1.8 GHz. (b) 2.2 GHz. (c) 2.6 GHz.

1.8, 2.2, and 2.6 GHz. The patterns at all the three frequencies keep a '∞' shape in the xz-plane, and an omnidirectional shape in the yz-plane. The simulated cross polarization is very small and is not observable in some cases. Figure 7 shows the results for port 2 excitation at frequencies of 1.8, 2.2, and 2.6 GHz. The patterns keep a '∞' shape in the yz-plane at all the three frequencies, while the patterns in the xz-plane change from an omnidirectional shape to a directional shape with the increase of frequency. The cross polarizations keep low in the xz-plane, but become high in the yz-plane with the increase of frequency. This may be caused by the asymmetry of the antenna structure. Owing that the radiation patterns of the co- and cross polarizations are uncorrelated [19], two independent channels can still be obtained. Therefore, this deterioration is acceptable in mobile communications.

The simulated and measured gains of the two modes are shown in Figure 8. Due to the limitation of measurement condition, the measured results are only given from 1.7 GHz to 2.7 GHz. It is shown that both the simulated and measured gains for port 1 and port 2 are around 3.5 dBi. The variation of the measured gains is larger than that of the simulated gains. However, the measured variation of gains is less than 2 dB over the entire bandwidth.

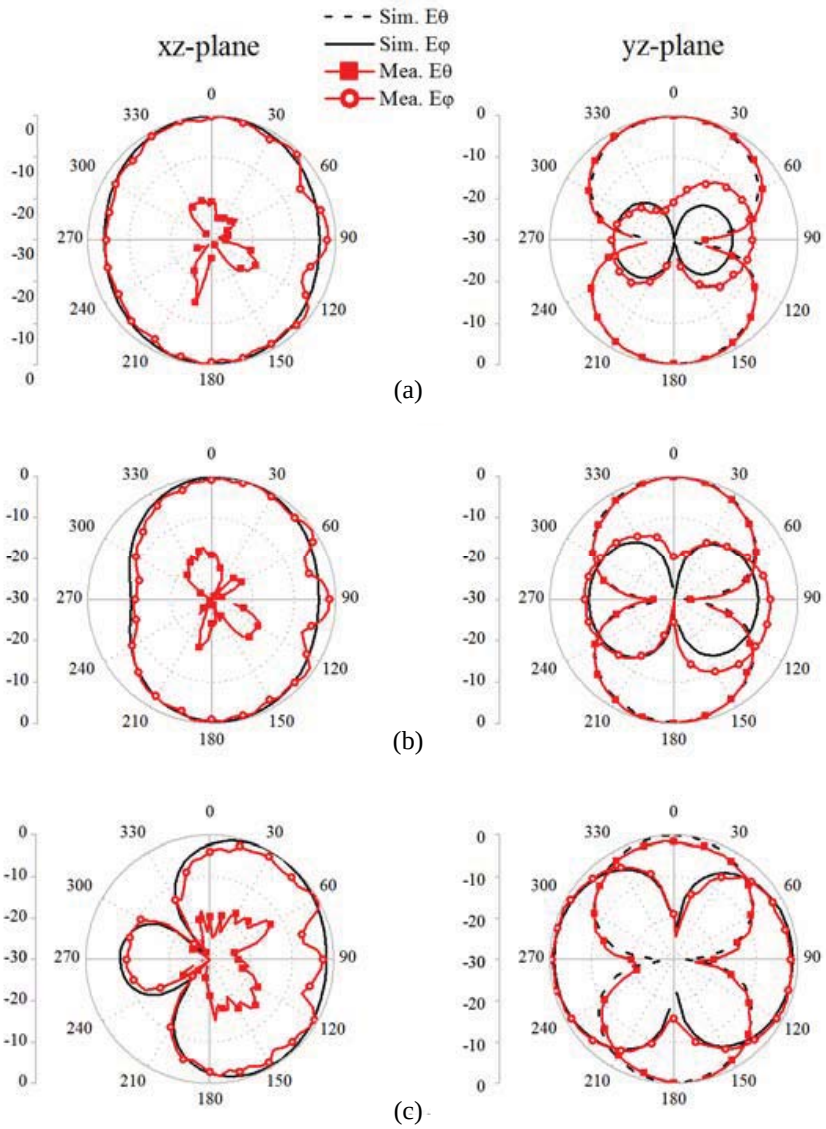

Figure 7. Simulated and measured normalized radiation patterns for port 2 excitation. (a) 1.8 GHz. (b) 2.2 GHz. (c) 2.6 GHz.

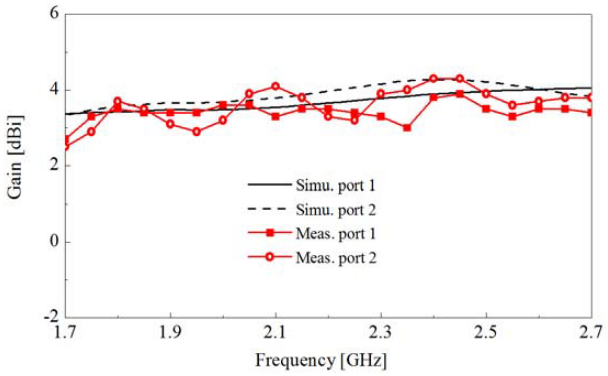

Figure 8. Simulated and measured gains of the proposed antenna.

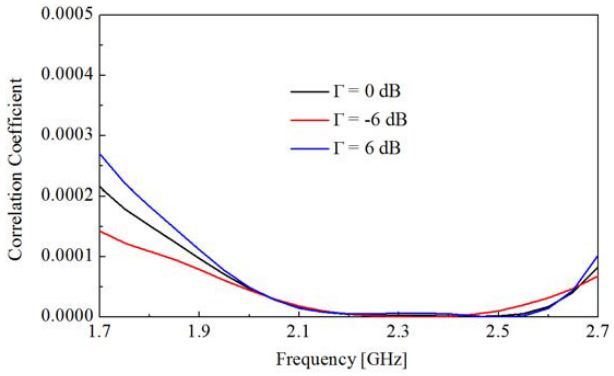

Figure 9. Simulated correlation coefficient with different Γ.

3.2. Diversity Performance

To evaluate the diversity performance of the proposed antenna, the correlation coefficient is analyzed based on the simulated far-field radiation results [22–24]. The envelope correlation coefficient (ρ_e) and the complex correlation coefficient (ρ_c) is defined as [23]

$$\rho_e \approx |\rho_c|^2 = \left| \frac{\oiint A_{12}(\Omega) d\Omega}{\sqrt{\oiint A_{11}(\Omega) d\Omega \cdot \oiint A_{22}(\Omega) d\Omega}} \right|^2 \tag{1}$$

where

$$A_{ij} = \Gamma \cdot E_{\theta,i}(\Omega) \cdot E^*_{\theta,i}(\Omega) \cdot p_\theta(\Omega) + E_{\varphi,i}(\Omega) \cdot E^*_{\varphi,j}(\Omega) \cdot p_\varphi(\Omega)$$

in which $E_{\theta,i}$ and $E_{\phi,i}$ are the θ and φ components of the far electrical field from the i-th antenna element. In this paper, $i = 1$ and 2 represent the vertical and the horizontal antenna elements, respectively. Γ is the average cross polarization ratio (XPR) of the environment, e.g., the power ratio of the vertical and horizontal polarizations, and $p_\theta(\Omega)$ and $p_\varphi(\Omega)$ are the angular density distribution of the incoming plane waves.

In the calculation, we adopted the uniformly angular density function in a full sphere for power density of the incident wave. In this distribution, three typical propagation environments are analyzed for the proposed antenna at the receiving end. For the case of $\Gamma = 6\,\text{dB}$ (or $-6\,\text{dB}$), the incident wave is mainly vertical (or horizontal) polarized, representing the urban microcell environment. For the case of $\Gamma = 0\,\text{dB}$, the vertical and horizontal polarized incident waves have equal power density, representing the indoor environment.

Figure 9 shows the simulated ρ_e with different Γ. The value of the correlation coefficient in all the cases is about 3×10^{-4} or less in the entire concerned frequency band. Thus, low correlation is obtained between the horizontal and vertical modes. Seen from the results, the horizontal and vertical modes of the loop antenna can be treated as two independent antennas with good diversity performance.

4. CONCLUSION

In this paper, a compact dual-polarized loop antenna is proposed. Two orthogonal one-wavelength-perimeter modes of the loop are excited by two simple feedings. Owing to the compact feeding structure and the loop mode, the proposed antenna occupies a small size of $58 \times 53\,\text{mm}^2$. The measured results show that the overlapping -10-dB bandwidth for both modes is 61.4%, covering the 1710–2690 MHz band. The measured ports isolation is about $-30\,\text{dB}$ over the entire bandwidth. With the advantages of compact size, broad bandwidth, high isolation, stable gains, and excellent diversity performance, the proposed dual-polarized loop antenna is suitable for mobile communication systems.

ACKNOWLEDGMENT

This work is supported by the National Basic Research Program of China under Contract 2013CB329002, in part by the National Natural Science Foundation of China under Contract 61301001, the National Science and Technology Major Project of the Ministry of Science and Technology of China 2013ZX03003008-002, the China Postdoctoral Science Foundation funded project 2013M530046, the Beijing Excellent Doctoral Dissertation Instructor project 20131000307.

REFERENCES

1. Wu, B. and K.-M. Luk, "A 4-port diversity antenna with high isolation for mobile communications," *IEEE Trans. Antennas Propag.*, Vol. 59, No. 5, 1660–1667, May 2011.
2. Zhang, S., B. K. Lau, A. Sunesson, and S. He, "Closely-packed UWB MIMO/diversity antenna with different patterns and polarizations for USB dongle applications," *IEEE Trans. Antennas Propag.*, Vol. 60, No. 9, 4372–4380, Sep. 2012.

3. Su, D., J. J. Qian, H. Yang, and D. Fu, "A novel broadband polarization diversity antenna using a cross-pair of folded dipoles," *IEEE Antennas Wireless Propag. Lett.*, Vol. 4, 433–435, 2005.
4. Wu, B. Q. and K. M. Luk, "A broadband dual-polarized magneto-electric dipole antenna with simple feeds," *IEEE Antennas Wireless Propag. Lett.*, Vol. 8, 60–63, 2009.
5. Liu, Y., H. Li, F. Wang, and S. Gong, "A novel miniaturized broadband dual-polarized dipole antenna for base station," *IEEE Antennas Wireless Propag. Lett.*, Vol. 12, 1335–1338, 2013.
6. Nguyen, V. A., R. S. Aziz, S. O. Park, and G. Yoon, "A design of multiband, dual-polarization, beam-switchable dual-antenna for indoor base stations," *Progress In Electromagnetics Research*, Vol. 149, 147–160, 2014.
7. Guo, Y. X., K. M. Luk, and K. F. Lee, "Broadband dual polarization patch element for cellular-phone base stations," *IEEE Trans. Antennas Propag.*, Vol. 50, No. 12, 251–253, Feb. 2002.
8. Gao, S., L. W. Li, M. S. Leong, and T. S. Yeo, "A broad-band dual-polarized microstrip patch antenna with aperture coupling," *IEEE Trans. Antennas Propag.*, Vol. 51, 898–900, Apr. 2003.
9. Deng, C., Y. Li, Z. Zhang, and Z. Feng, "A wideband high-isolated dual-polarized patch antenna using two different balun feedings," *IEEE Antennas Wireless Propag. Lett.*, Vol. 13, 1617–1619, 2014.
10. Peng, H.-L., W.-Y. Yin, J.-F. Mao, D. Huo, X. Hang, and L. Zhou, "A compact dual-polarized broadband antenna with hybrid beam-forming capabilities," *Progress In Electromagnetics Research*, Vol. 118, 253–271, 2011.
11. Secmen, M. and A. Hizal, "A dual-polarized wide-band patch antenna for indoor mobile communication applications," *Progress In Electromagnetics Research*, Vol. 100, 189–200, 2010.
12. Moradi, K. and S. Nikmehr, "A dual-band dual-polarized microstrip array antenna for base stations," *Progress In Electromagnetics Research*, Vol. 123, 527–541, 2012.
13. Xie, J.-J., Y.-Z. Yin, J. Ren, and T. Wang, "A wideband dual-polarized patch antenna with electric probe and magnetic loop feeds," *Progress In Electromagnetics Research*, Vol. 132, 499–515, 2012.
14. Huang, C. Y., T. W. Chiou, and K. L. Wong, "Dual-polarized dielectric resonator antennas," *Microw. Opt. Technol. Lett.*, Vol. 31, 222–223, 2001.
15. Gao, Y., Z. Feng, and L. Zhang, "Compact CPW-fed dielectric resonator antenna with dual polarization," *IEEE Antennas Wireless Propag.*, Vol. 10, 544–547, 2011.
16. Soliman, E. A., M. S. Ibrahim, and A. K. Abdelmageed, "Dual-polarized omnidirectional planar slot antenna for WLAN applications," *IEEE Trans. Antennas Propag.*, Vol. 53, No. 9, 3093–3097, Sep. 2005.
17. Hsuan, L. C., C. S. Yuan, and H. Powen, "Isosceles triangular slot antenna for broadband dual polarization applications," *IEEE Trans. Antennas Propag.*, Vol. 57, No. 10, 3347–3351, Oct. 2009.
18. Li, Y., Z. Zhang, W. Chen, Z. Feng, and M. F. Iskander, "A dual-polarization slot antenna using a compact CPW feeding structure," *IEEE Antennas Wireless Propag. Lett.*, Vol. 9, 191–194, 2010.
19. Jiang, X., Z. Zhang, Y. Li, and Z. Feng, "A wideband dual-polarized slot antenna," *IEEE Antennas Wireless Propag. Lett.*, Vol. 12, 1010–1013, 2013.
20. Baek, S. and S. Lim, "Compact planar MIMO antenna array with polarisation diversity on single layer," *Electron. Lett.*, Vol. 46, No. 13, 880–882, Jun. 2010.
21. Li, Y., Z. Zhang, W. Chen, Z. Feng, and M. F. Iskander, "Dual-mode loop antenna with compact feed for polarization diversity," *IEEE Antennas Wireless Propag. Lett.*, Vol. 10, 95–98, 2011.
22. Vaughan, R. and J. Andersen, "Antenna diversity in mobile communications," *IEEE Trans. Veh. Technol.*, Vol. 36, No. 4, 149–172, Nov. 1987.
23. Gao, Y., X. chen, Z. Ying, and C. Parini, "Design and performance investigation of a dual-element PIFA array at 2.5 GHz for MIMO terminal," *IEEE Trans. Antennas Propag.*, Vol. 55, No. 12, 3422–3440, Dec. 2007.
24. Li, Y., Z. Zhang, J. Zheng, and Z. Feng, "Compact azimuthal omnidirectional dual-polarized antenna using highly isolated colocated slots," *IEEE Trans. Antennas Propag.*, Vol. 60, No. 9, 4037–4045, Sep. 2012.